Electronic Supplementary Material (ESI) for Physical Chemistry Chemical Physics.

SUPPORTING INFORMATION

Amphiphilic Ionic Liquid Induced Fusion of Phospholipid Liposomes

Sandeep Kumar [a], Navleen Kaur [a] and Venus Singh Mithu* [a]

[a]Department of Chemistry, Guru Nanak Dev University, Amritsar-143005, India

AUTHOR INFORMATION

Corresponding Author:

venus.chem@gndu.ac.in

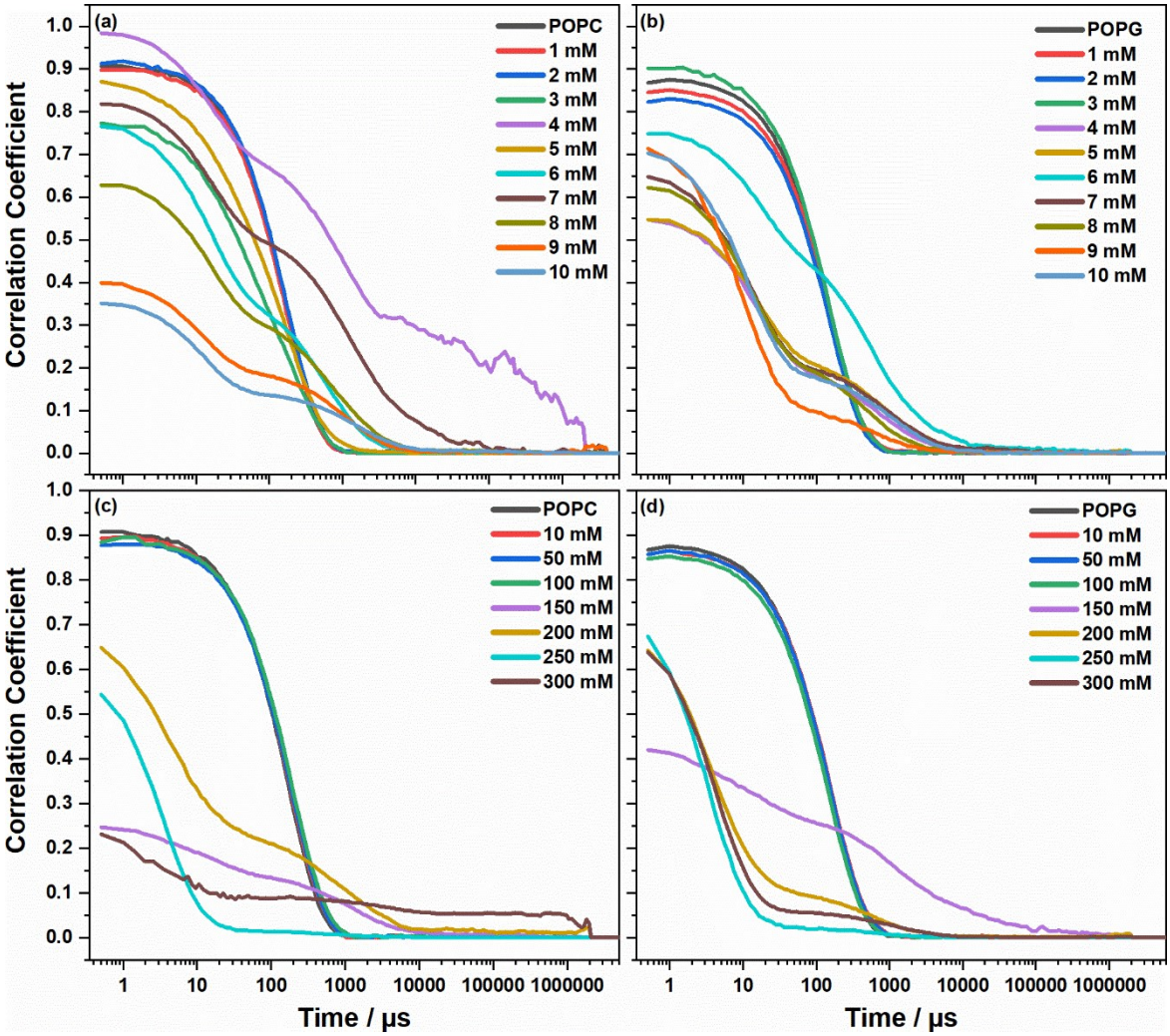

Figure S1. Correlation coefficients for (a, c) POPC and (b, d) POPG LUVs in the absence and presence of ionic liquids (a, b) $[C_{12}MIM]^+Br^-$ and (b, d) $[C_8MIM]^+Br^-$ at various concentrations at 25°C.

Impact of Triton X-100 on the fluorescence intensity of NBD-PE

To determine the impact of Triton X-100 on the fluorescence intensity vesicles (POPC) containing 1.5 mol% NBD-PE molecules. The fluorescence intensity of NBD was monitored in the absence and presence of 1% Triton X 100 (v/v). The fluorescence emission was measured at 535 nm with the excitation wavelength set at 460 nm. The fluorescence intensity of pure NBD-PE was normalised with respect to the maximum fluorescence intensity obtained in the presence of 1% Triton X-100 (v/v). So, Triton X-100 quenching correction factor (TQ) calculated from **Figure S1** came out to be ~ 1.45. This is the main reason for multiplying the observed fluorescence intensity of NBD with 1.45 in the presence of Triton X-100.

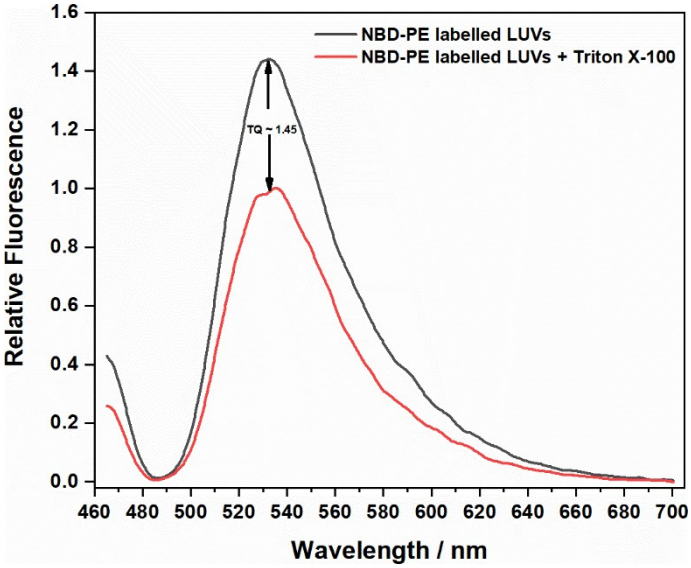

Figure S2. Relative fluorescence intensity of POPC LUVs containing 1.5 mol% NBD-PE in absence (black line) and presence (red line) of 1% Triton X-100.

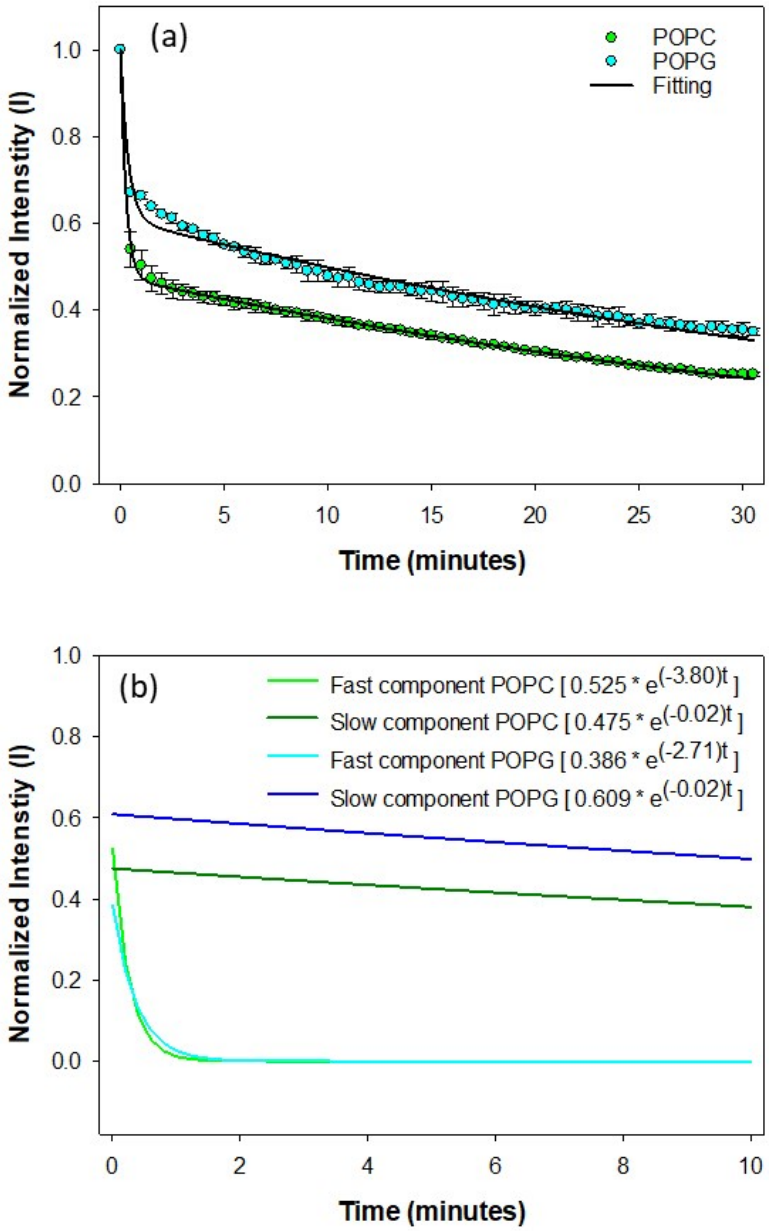

Figure S3: Control experiment showing dithionite bleaching of POPC or POPG vesicles containing 1.5 mol% of the fluorescent NBD-PE. This control experiment exhibits selective silencing of NBD molecules in the outer leaflet (OL). Clearly, dithionite quenching exhibits two time constants: a very rapid quenching (seconds) and a very slow quenching (minutes). These time constants were extracted by fitting the normalized fluorescence intensity (I) to a biexponential decay function ($I = a_1 e^{-k_1 t} + a_2 e^{-k_2 t}$). (b) Both slow and fast components plotted as a function of time. The fast component decays within 2 minutes of dithionite exposure corresponding to a total quenching to ~55 % in POPC and ~40% in POPG LUVs. This percentage corresponds to the fraction of NBD-PE molecules present in the OL of LUVs.

Determination of critical micelles concentration of ionic liquids

CMC values of $[C_nMIM]^+Br^-$ (n = 8, 12) were determined using steady state fluorescence studies using PerkinElmer LS-55 Luminescence spectrometer. All measurements were performed at 298.15 K using pyrene[1] dye (2μM) as an external fluorescent probe. The emission spectrum was recorded in the range 350-450 nm keeping the excitation wavelength fixed at 335 nm, and slit width at 3.0 nm in each case. The ratio of intensity of first (I_1) to third (I_3) vibration bands of pyrene was plotted as a function of ionic liquid concentration to obtain CMC values of 3.3 mM ($[C_{12}MIM]^+Br^-$, **Figure S4**) and 48 mM ($[C_8MIM]^+Br^-$, **Figure S5**) in 7.7 mM Tris HCl buffer containing 100 mM NaCl.

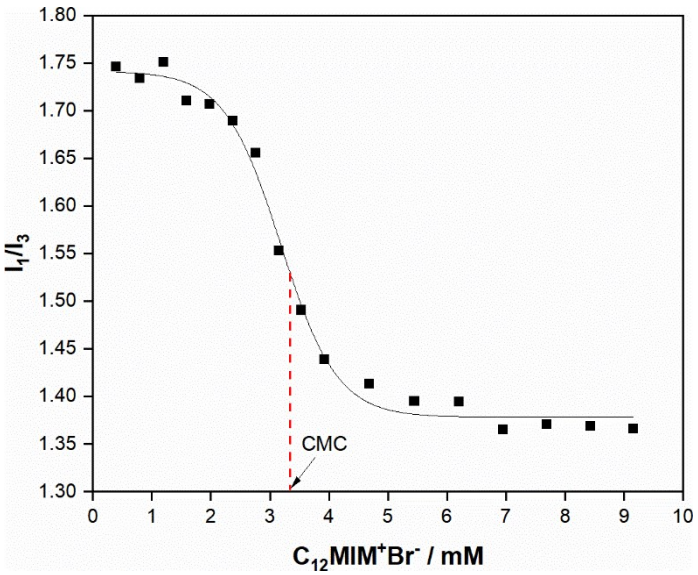

Figure S4. Ratio of intensity of first (I_1) to third (I_3) vibration bands of pyrene (I_1/I_3) plotted as a function of $[C_{12}MIM]^+Br^-$ concentrations. The value where I_1/I_3 value is reduced to half of its starting value is taken as CMC.

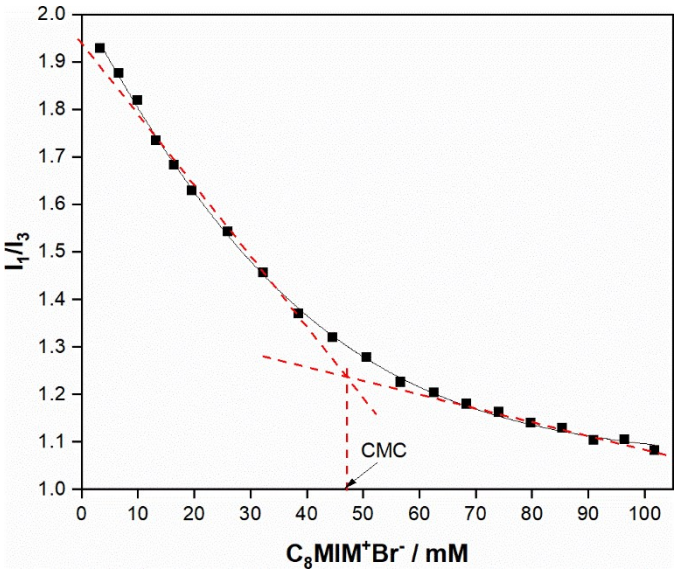

Figure S5. Ratio of intensity of first (I_1) to third (I_3) vibration bands of pyrene (I_1/I_3) plotted as a function of $[C_8MIM]^+Br^-$ concentrations

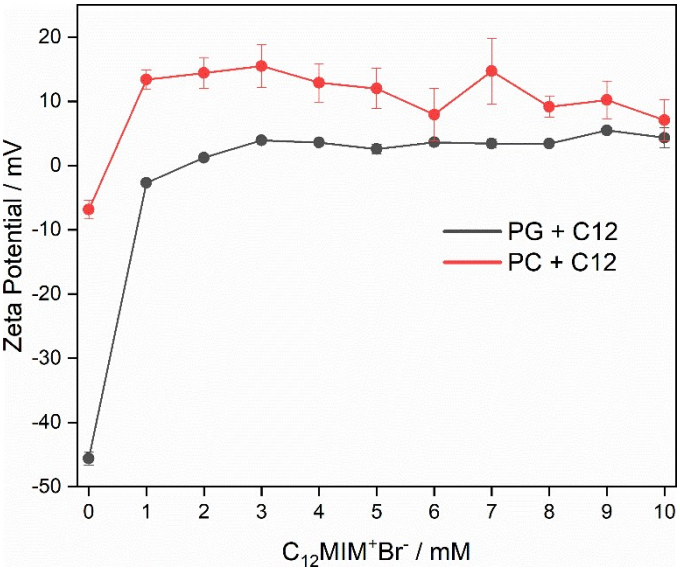

Figure S6. The change in zeta potential of POPC and POPG LUVs as function of $[C_{12}MIM]^{+}Br^{-}$ concentration.

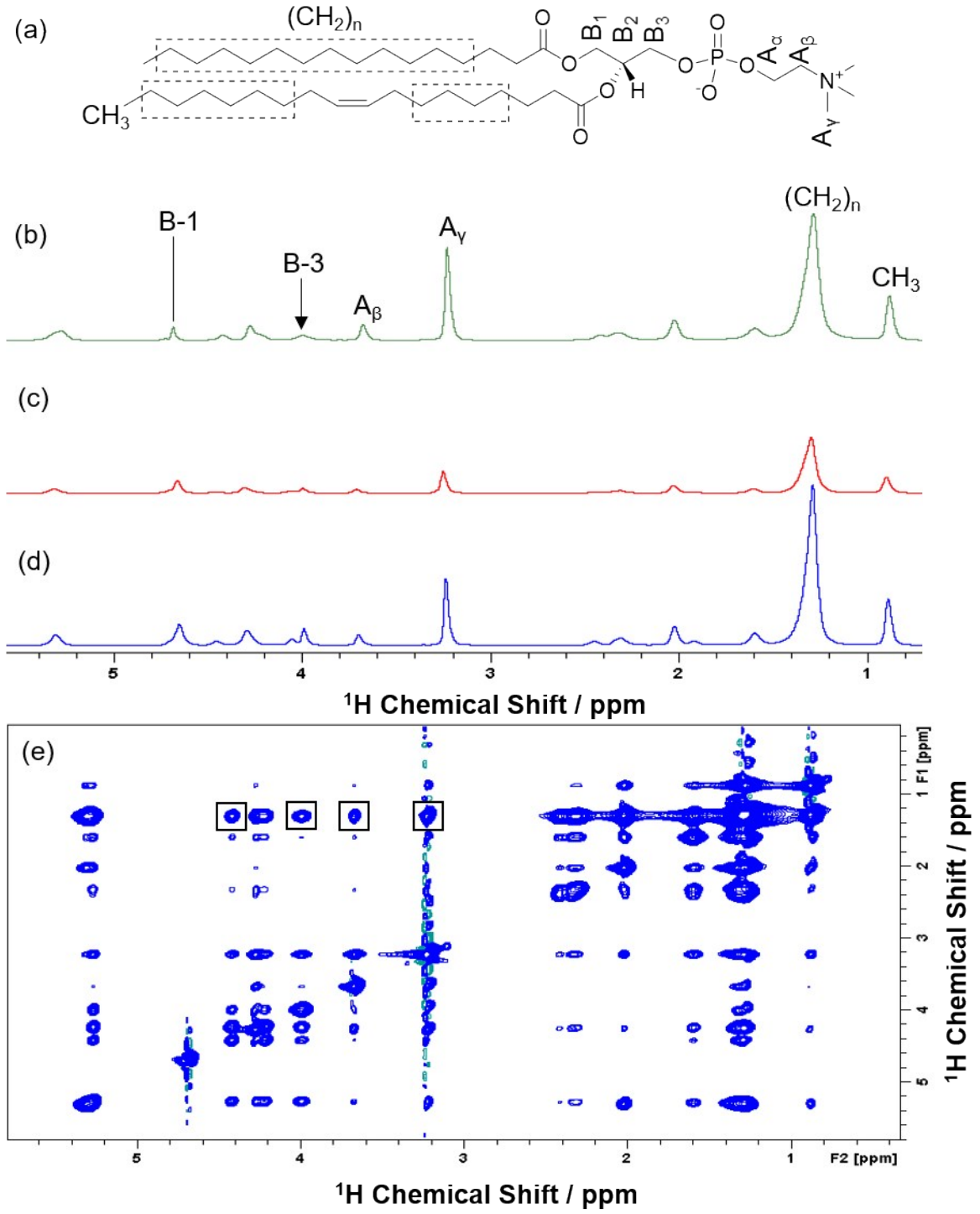

Figure S7. (a) Molecular structures of POPC including the nomenclature. (b) ^{1}H MAS NMR spectra of POPC bilayer along with peak assignment. ^{1}H MAS NMR spectra of POPC in presence of (c) $C_8MIM^+Br^-$ and (d) $C_{12}MIM^+Br^-$. (e) ^{1}H-^{1}H NOESY NMR spectrum of POPC at a mixing time of 300 ms. The cross peaks between the -$(CH_2)_n$- protons of lipid chain and the protons of lipid head group which were used in the analysis are indicated by black squares.

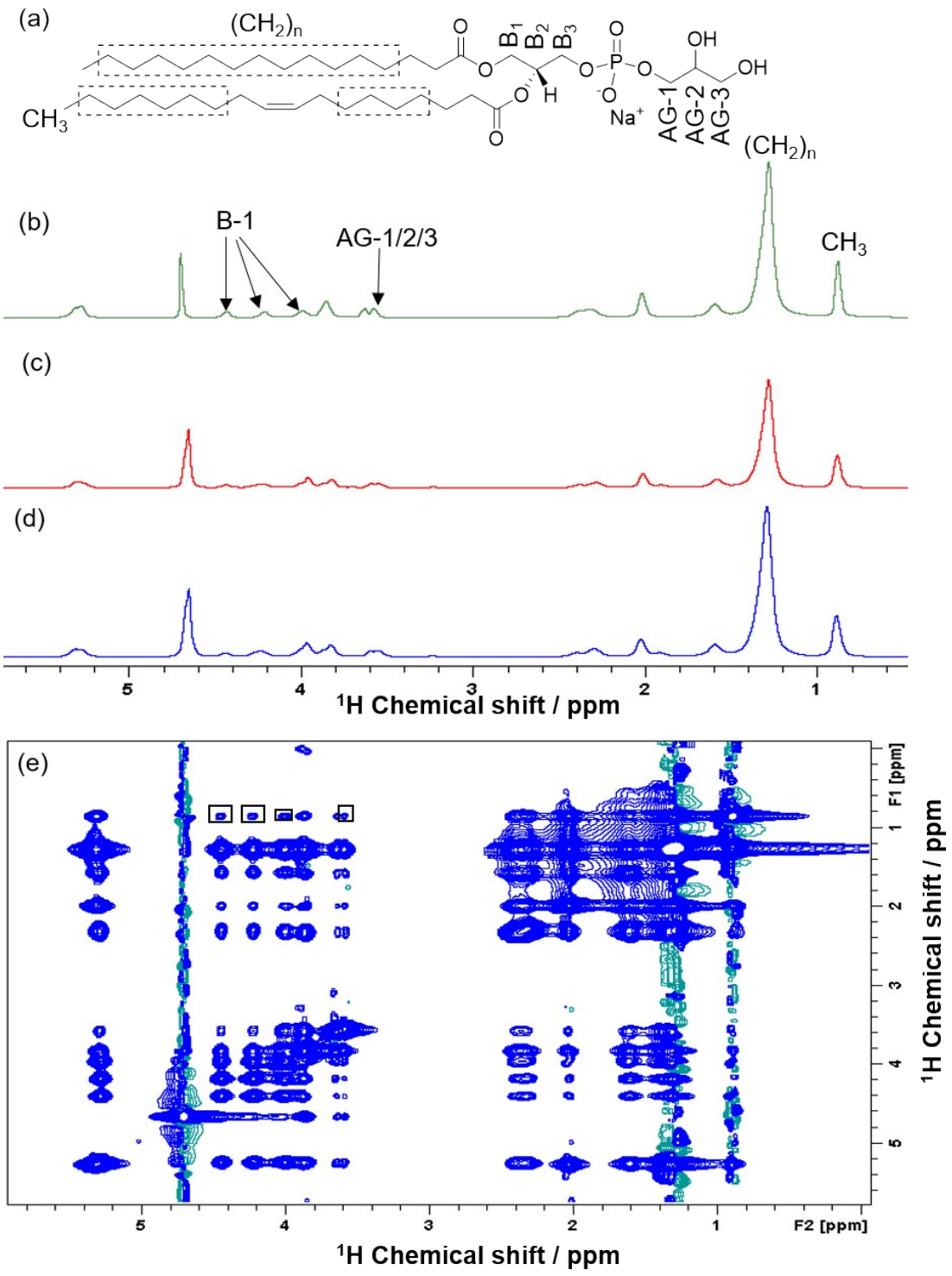

Figure S8. (a) Molecular structures of POPG including the nomenclature. (b) ^{1}H MAS NMR spectra of POPG bilayer along with peak assignment. ^{1}H MAS NMR spectra of POPG in presence of (c) $C_8MIM^+Br^-$ and (d) $C_{12}MIM^+Br^-$. (e) ^{1}H-^{1}H NOESY NMR spectrum of POPG at a mixing time of 300 ms. The cross peaks between the -$(CH_2)_n$- protons of lipid chain and the protons of lipid head group which were used in the analysis are indicated by black squares.

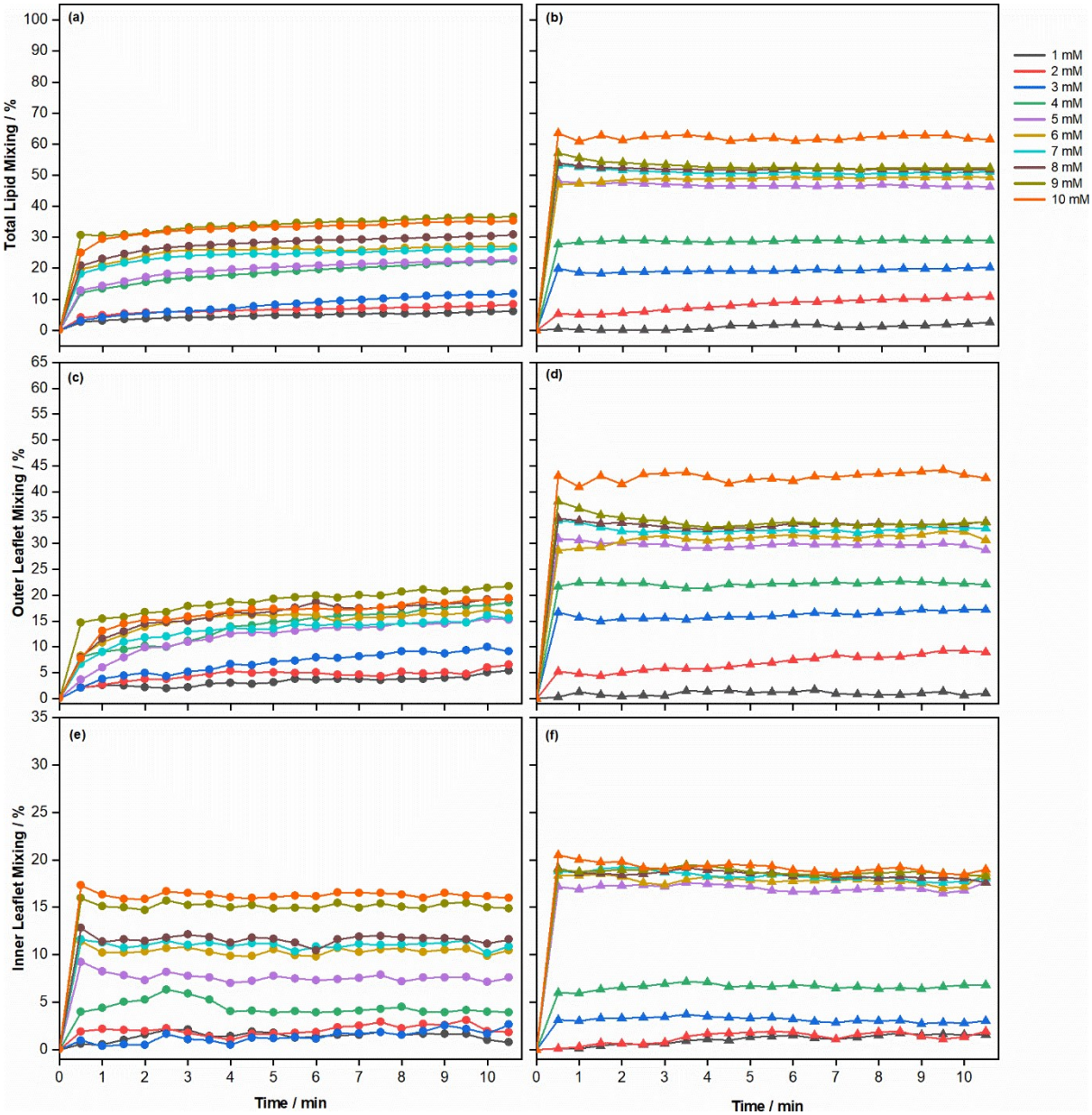

Figure S9: Time course of percentage of (a, b) total lipid mixing, and (c, d) OL mixing, and (e, f) IL mixing in (a, c and e) POPC, and (b, d, and f) POPG LUVs upon adding $C_{12}MIM^{+}Br^{-}$ in concentrations as indicated in legend. The experimental error for each measurement is not more than 3%.

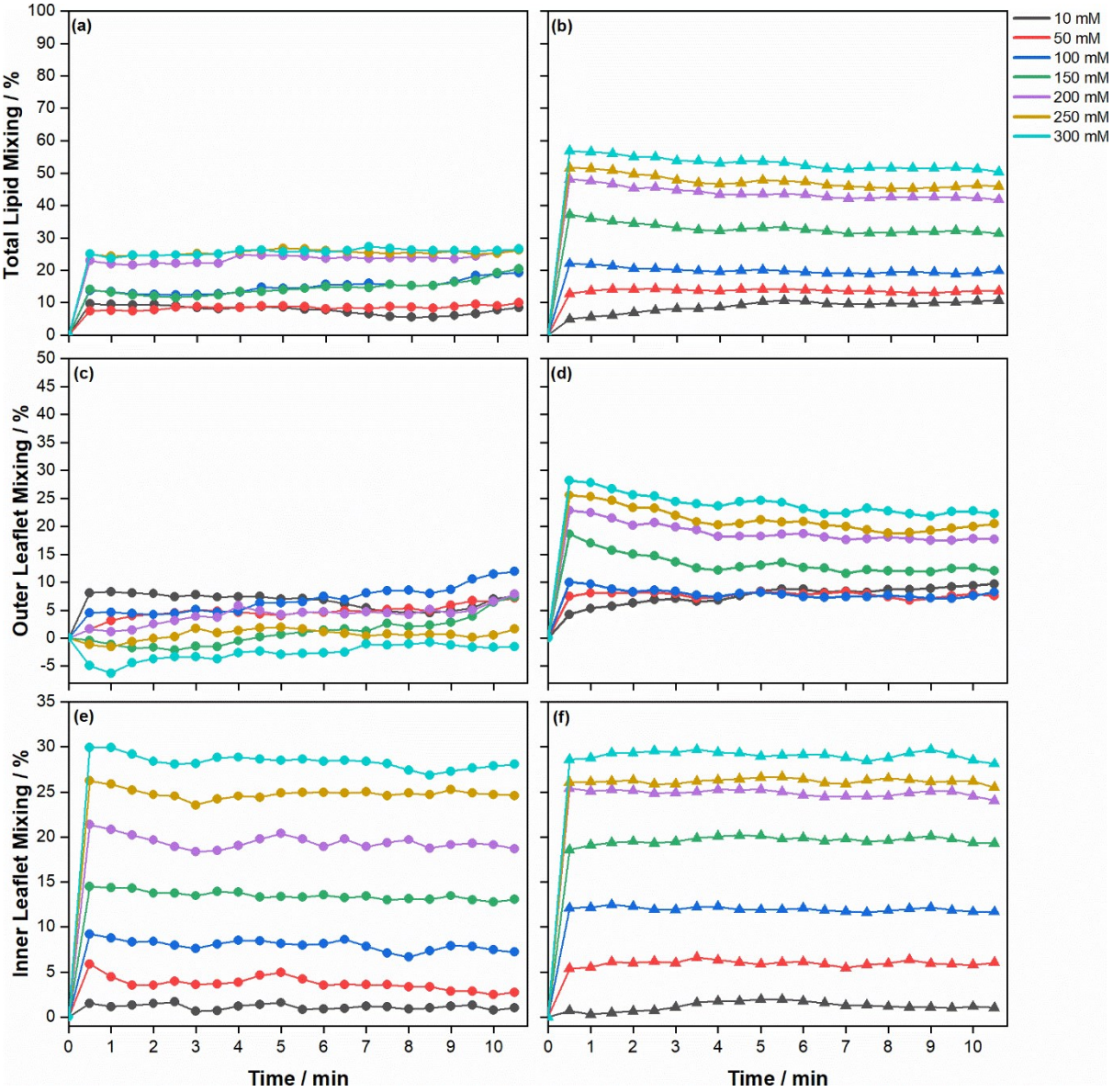

Figure S10: Time course of percentage of (a, b) total lipid mixing, and (c, d) OL mixing, and (e, f) IL mixing in (a, c, and e) POPC, and (b, d, and f) POPG LUVs upon adding $C_8MIM^+Br^-$ in concentrations as indicated in legend. The experimental error for each measurement is not more than 3%.

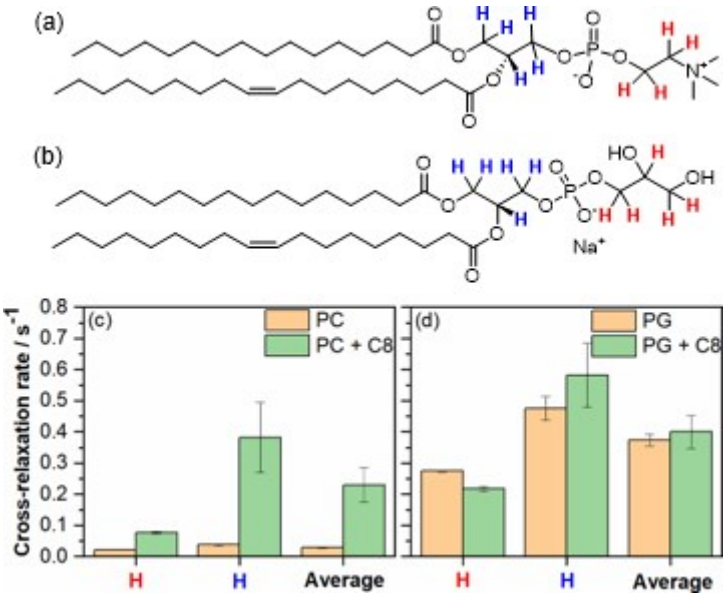

Figure S11: Structures of (a) POPC and (b) POPG molecules with protons in the glycerol and head-group region highlighted in blue and red colours, respectively. ^{1}H-^{1}H NOESY average cross-relaxation rates between these protons and -$(CH_2)_n$- protons in lipid chains of (c) POPC and (d) POPG observed in the absence and presence of $[C_8MIM]^+Br^-$. Also shown are the average cross-relaxation rates glycerol and head-group protons taken together.

REFERENCE

1. K. Ananthapadmanabhan, E. Goddard, N. Turro and P. L. Kuo, *Langmuir*, 1985, **1**, 352-355.